NITROGEN CONTROL DURING THE AUTOGENOUS ARC WELDING OF STAINLESS STEEL

M. Du Toit and P.C. Pistorius
University of Pretoria (South Africa)

ABSTRACT

This study deals with nitrogen absorption and desorption during the autogenous welding of stainless steel, investigating the influence of the base metal nitrogen and surface-active element concentrations and nitrogen partial pressure in the shielding gas. The weld nitrogen concentration increases with shielding gas nitrogen content at low nitrogen partial pressures, but at higher partial pressures nitrogen absorption is balanced by N_2 evolution. This steady-state nitrogen content is not influenced significantly by the base metal nitrogen content in low sulphur alloys, but in high sulphur alloys, an increase in the initial nitrogen concentration causes higher weld nitrogen contents over the entire range of partial pressures evaluated. The weld metal saturation limit is reached at progressively lower shielding gas nitrogen contents as the base metal nitrogen level increases. It is postulated that less nitrogen is required in the shielding gas to reach the saturation limit in the high sulphur alloys because an appreciable fraction of the nitrogen already present in the base metal is prevented from escaping by a higher level of surface coverage. A kinetic model can be used to describe this behaviour. The desorption rate constant decreases with an increase in sulphur content, but the absorption rate constant is not a strong function of the sulphur concentration. The higher rate of nitrogen removal at the onset of steady-state behaviour causes higher-nitrogen alloys to require more supersaturation prior to bubble formation.

IIW-Thesaurus keywords: *Stainless steels; Austenitic stainless steels; Arc welding; Alloying additions; N additions; Sulphur; Chemical composition; Parent materials; Weld metal; Influencing factors; Shielding gases; Gases; Mixtures; Nitrogen; Absorption; Outgassing; Pressure; Reaction kinetics; Mathematical models; Practical investigations; Reference lists.*

1 INTRODUCTION

In mild steel, low alloy steel and ferritic stainless steel, nitrogen is generally considered an undesirable impurity, causing porosity and the formation of brittle nitrides [1]. In austenitic and duplex austenitic-ferritic stainless steels, however, nitrogen is often a valued alloying element. In part, this has stemmed from the desire to use nitrogen as a substitute for nickel, thereby reducing alloying element costs. In addition to the fact that the consumption of an expensive strategic metal is reduced, nitrogen is considered to be as much as thirty times as powerful as nickel as an austenite-former [2-3]. Nitrogen is also an excellent solid solution strengthening element in stainless steel, increasing the yield strength at room temperature and at sub-zero temperatures [4-5], with no significant decrease in toughness or ductility [5-6]. Nitrogen-alloyed austenitic stainless steels therefore offer a unique combination of strength and toughness. Nitrogen is also reported to improve the passivation characteristics of stainless steels. It increases resistance to localised corrosion [7-8], and reduces sensitisation effects during welding [9-10].

Doc. IIW-1618-03 (ex-doc. IX-H-565-03 / IX-2068-03) recommended for publication by Commission IX "Behaviour of metals subjected to welding"

In order to realise the advantages associated with nitrogen alloying, the nitrogen has to be in solution in the metal matrix. Excess nitrogen tends to cause porosity or form brittle nitrides. Iron, mild steel and low alloy steel have low solubility limits for nitrogen (the equilibrium solubility of nitrogen in iron at its melting point is only approximately 0.044 per cent (by mass) at 1 atmosphere pressure [11]). It is therefore important to limit nitrogen contamination in these steels. This poses a particular problem during welding, where nitrogen from the surrounding atmosphere can be absorbed by the weld metal in spite of the precautions normally taken to shield the arc and the weld pool. Austenitic stainless steels can accommodate significantly higher levels of nitrogen in solution. In nitrogen-alloyed austenitic stainless steels, the most important problem during welding is often not nitrogen absorption, but nitrogen desorption to the arc atmosphere, resulting in lower nitrogen levels in the weld metal. A decrease in nitrogen concentration in the region of the weld has a detrimental effect on the mechanical properties and corrosion resistance of the joint.

In order to control nitrogen absorption and evolution from the molten pool during welding, fundamental knowledge of the absorption and desorption mechanisms is essential. Over the past years a number of studies have dealt with arc melting experiments under static condi-

tions (stationary arc), while others concerned experiments under more realistic welding conditions (travelling arc). The results of these studies show that nitrogen absorption and desorption are complex phenomena, influenced by many factors. Some of these investigations are briefly considered below.

The equilibrium solubility of nitrogen in iron is governed by Sievert's law, which states that the nitrogen concentration in liquid iron is proportional to the square root of the nitrogen partial pressure above the melt. Sievert's law implies that the nitrogen solubility limit in iron alloys can be raised by increasing the partial pressure of the diatomic gas above the melt. This approach has been proposed for reducing nitrogen losses and for preventing nitrogen-induced porosity during the welding of nitrogen-containing austenitic stainless steels. The majority of researchers, however, agree that Sievert's law cannot be applied to describe the dissolution of a diatomic gas in liquid metal in the presence of a plasma [12-16]. Such a plasma phase resides above the weld pool during most fusion welding processes. Reported weld nitrogen contents generally exceed the concentrations predicted from equilibrium considerations. As shown schematically in Fig. 1, the weld nitrogen content is reported to increase with an increase in the nitrogen partial pressure, PN_2, at low partial pressures. At higher shielding gas nitrogen contents, the weld nitrogen concentration assumes a constant steady-state value that is independent of the actual partial pressure. At this point a dynamic balance is established and the rate of nitrogen absorption at the weld surface is balanced by bubble formation in the melt.

The majority of authors attribute the enhanced solubility in the presence of a plasma to the existence of monatomic nitrogen, N, in the arc [16-19]. These nitrogen atoms form as diatomic nitrogen molecules partially dissociate in the high temperature arc. Gedeon and Eager [18-19] proposed a two-step absorption process, in which hydrogen (also a diatomic molecule) dissociates in the high temperature regions of the arc, followed by

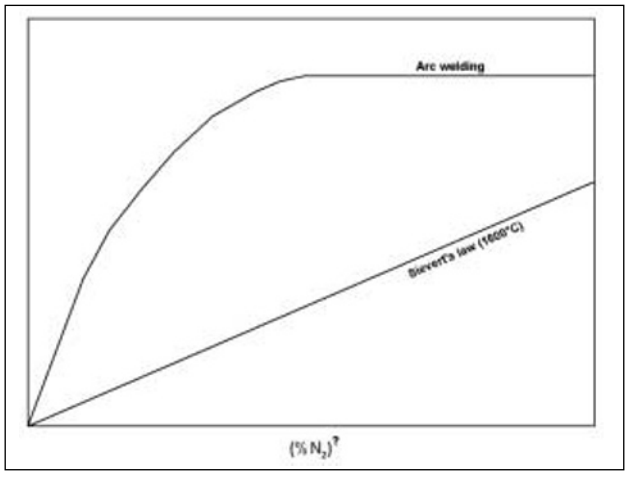

Fig. 1. Schematic illustration of the weld metal nitrogen concentration as a function of the square root of the nitrogen partial pressure in the shielding gas.

absorption at the weld pool surface. Their thermodynamic model was subsequently modified by Mundra and DebRoy [20] and Palmer and DebRoy [21] to describe the dissolution of nitrogen in welds. The authors defined a hypothetical dissociation temperature, T_d, at which the equilibrium dissociation of diatomic nitrogen produces the actual partial pressure of monatomic nitrogen present in the plasma. The monatomic nitrogen in the arc plasma then dissolves in the weld metal at the weld pool surface temperature, T_s.

This model does not take into account the weld composition, which has a significant effect on the solubility of nitrogen in iron [22-23]. Kuwana *et al.* [24] addressed this in the form of a thermodynamic model developed to predict nitrogen solubilities in stainless steel welds during autogenous welding. The authors reported that the weld nitrogen content is a function of the chromium content of the base metal. Chromium appears to increase the equilibrium nitrogen solubility and the time required to reach this equilibrium value. In low chromium alloys, the weld nitrogen concentration approaches the equilibrium solubility, but enough time may not be available during welding for nitrogen absorption to increase the weld nitrogen content to a level approaching the equilibrium value in high chromium steels.

These results suggest that a kinetic approach may be more appropriate for describing the dissolution of nitrogen in stainless steels. Katz and King [16] studied nitrogen absorption and desorption kinetics during the arc melting of iron and observed both first- and second-order kinetics, depending on the composition, and in particular the surface-active element concentration, of the alloy. Alloys containing high levels of surface-active elements displayed second-order desorption kinetics, whereas alloys with low concentrations of these elements displayed first-order kinetics. The Katz and King kinetic model, however, does not address the influence of alloying elements or welding parameters.

Nitrogen absorption and desorption during the autogenous welding of nitrogen-alloyed stainless steels is expected to be a function of the base metal nitrogen content prior to welding and the weld surface-active element concentration. Limited information is available describing the influence of the base metal nitrogen content on nitrogen dissolution in iron alloy welds. Okagawa *et al.* [6] and Suutala [25] studied autogenous gas tungsten arc (GTA) welds in a number of austenitic stainless steels with nitrogen levels varying between 0.008 and 0.076 per cent and concluded that base metal nitrogen does not take part in the nitrogen dissolution reaction during welding. Arata *et al.* [26] reported that the total weld nitrogen content is the sum of the residual nitrogen content of the base metal and any nitrogen picked up from the shielding gas. The nitrogen levels of the steels investigated by these authors were relatively low compared to those of nitrogen-alloyed austenitic stainless steels, and were probably well below the nitrogen solubility limit of the weld metal. For this reason it is unlikely that their conclusions can be extended to the case of high nitrogen alloys.

Ample evidence exists to show that the presence of surface-active elements, in particular sulphur and oxygen, has a significant influence on nitrogen dissolution in iron alloy welds. Lancaster [1] reported that the amount of nitrogen absorbed during arc welding increases in the presence of oxygen, and Ogawa *et al.* [27] demonstrated that nitrogen-induced porosity in austenitic stainless steel welds can be curbed by welding in an atmosphere containing a small amount of oxidising gas. According to Blake [11], the presence of oxygen leads to lower nitrogen desorption rates and Uda and Ohno [28] reported that the presence of surface-active elements markedly increases the nitrogen content of iron and the level of supersaturation in welds. Sinha and Gupta [29] observed that the nitrogen absorption rate in stainless steel decreases in the presence of surface-active elements. The most likely explanation for the influence of surface-active elements is that these elements occupy a fraction of the available surface sites, making it more difficult for nitrogen to adsorb on or desorb from the metal surface [16].

2 OBJECTIVES OF THE INVESTIGATION

As demonstrated above, the absorption and desorption of nitrogen during welding are complex phenomena influenced by many factors, including the nature of the species present in the arc plasma, the weld metal alloying content and the welding parameters. No unified theory for the quantitative understanding of the extent of enhanced dissolution in stainless steels has emerged up to this point. Most of the theoretical models currently available in literature describe nitrogen absorption and desorption from autogenous iron or carbon steel welds and may not be appropriate for describing these processes in more highly alloyed stainless steel welds.

This investigation aimed at examining the influence of the following factors on the absorption and desorption of nitrogen during the autogenous welding of stainless steel:

– shielding gas composition,
– base metal nitrogen content prior to welding, and
– surface-active element concentration in the weld metal.

These variables were selected to quantify the role of certain factors not addressed in currently available literature, to clarify inconsistencies in the existing literature, and to investigate the interaction between these variables in practice.

In order to examine the influence of each of these factors on the nitrogen content of stainless steel welds, the compositions of the parent metal and the shielding gas were adjusted to produce an experimental matrix quantifying the influence of each variable individually and in combination. The same welding parameters (welding current, arc length, travel speed and shielding gas flow rate) were used during all the experiments, except where otherwise indicated, to avoid the introduction of too many variables. Following the experimental work, a kinetic model was derived to explain the results obtained and to serve as a basis for further modelling work.

3 EXPERIMENTAL PROCEDURE

3.1 Stainless steel alloys studied

During the course of this investigation, the influence of autogenous welding on the nitrogen content of six experimental stainless steel alloys was evaluated. The chemical compositions of these alloys are shown in Table 1. The experimental alloys were designed to have compositions similar to that of type AISI 310 stainless steel, a highly alloyed austenitic material that is normally produced without any deliberate nitrogen addition. This steel was selected as the base alloy for this investigation because it solidifies as austenite and remains fully austenitic down to room temperature. This prevents any bulk solid-state phase transformations, which may lead to changes in the solid-state nitrogen solubility in the alloy, from taking place after solidification.

In order to study the influence of the original base metal nitrogen content on nitrogen absorption and desorption during welding, the experimental alloys were produced with three nitrogen concentrations:

– a *low* nitrogen level (residual nitrogen content of approximately 0.005%),
– a *medium* nitrogen level (approximately 0.1%), and
– a *high* nitrogen level (approximately 0.25%). This nitrogen level corresponds to the equilibrium nitrogen solubility limit in these steels calculated at a temperature of 1,600°C and a nitrogen pressure of 1 atmosphere [23].

The influence of the surface-active element concentration on nitrogen absorption and desorption during welding was evaluated by producing each of the *low*, *medium* and *high* nitrogen experimental alloys described above with two different sulphur concentrations:

– a *low* sulphur content (approximately 0.02%), and
– a *high* sulphur content (approximately 0.05%).

Table 1. Chemical compositions of the stainless steel alloys investigated (percentage by mass, balance iron).

Alloy	Comments	Cr	Ni	Mn	Si	C	S	N
VFA 657	Low N, low S	24.4	20.1	1.91	1.60	0.075	**0.023**	**0.005**
VFA 658	Medium N, low S	24.6	19.9	1.89	1.63	0.080	**0.023**	**0.105**
VFA 659	High N, low S	24.3	19.9	1.93	1.63	0.085	**0.022**	**0.240**
VFA 752	Low N, high S	24.6	19.5	1.99	1.51	0.087	**0.052**	**0.006**
VFA 753	Medium N, high S	24.5	19.3	1.89	1.61	0.082	**0.061**	**0.097**
VFA 755	High N, high S	24.5	19.3	1.90	1.55	0.079	**0.049**	**0.280**

The *low* sulphur level shown above falls well within the specified sulphur concentration range for type AISI 310 stainless steel. As an alternative to varying the sulphur content of the base metal, small amounts of oxygen can be added to the shielding gas during welding, thereby varying the absorbed oxygen content of the weld metal. Varying the sulphur content of the base metal was preferred during this investigation because it provides more accurate control of the surface-active element concentration of the weld metal.

3.2 Welding procedure

All the stainless steel samples were hot rolled to a thickness of 6 mm, thoroughly ground to remove any scale or surface oxides and degreased using acetone. The samples were then welded in an enclosed glove box using an automatic autogenous gas tungsten arc (GTA) welding process. Direct current electrode negative polarity and a 2% thoriated tungsten electrode were used. In order to prevent contamination from the atmosphere due to air entrapment in the arc, the glove box was flushed with pure argon for at least fifteen minutes prior to welding, and a low argon flow rate was maintained through the box during welding to ensure a slight positive pressure inside the glove box. Shielding was supplied by shielding gas flowing through the welding torch at a pressure of 1 atmosphere and a flow rate of 20 ℓ/minute. Welding was performed using a current of 150 A, an arc length of 2 mm and a welding speed of 2.7 mm/s. Pure argon and four premixed shielding gases, listed below, were used to evaluate the influence of nitrogen additions to argon shielding gas on the absorption and desorption of nitrogen:

– pure argon,
– argon – 1.09% N_2,
– argon – 5.3% N_2,
– argon – 9.8% N_2, and
– argon – 24.5% N_2.

All the stainless steel alloys listed in Table 1 were welded using these shielding gases and welding parameters. After welding the nitrogen content of each weld was analysed using an inert gas fusion analysis technique, taking care to remove the metal drillings required for analysis only from the weld. At least two analyses were performed on each sample to ensure adequate repeatability.

3.3 Bubble formation in the weld pool during welding

As stated earlier, the weld metal nitrogen content usually increases rapidly with an increase in the shielding gas nitrogen content at low nitrogen partial pressures, followed by steady-state behaviour where nitrogen absorption from the arc is balanced by nitrogen evolution from the weld pool. This steady-state region is associated with violent degassing and nitrogen bubble formation. In order to prevent severe nitrogen losses from nitrogen-alloyed stainless steels and to prevent the formation of nitrogen-induced porosity in welds, shielding gas nitrogen contents associated with steady-state behaviour must be avoided. The shielding gas nitrogen content at the onset of bubble formation was determined for each of the alloys listed in Table 1 by using a range of argon-nitrogen shielding gases, mixed using a system of flow meters. The flow meters were calibrated to supply shielding gas with the desired argon-nitrogen ratio at a total flow rate of 20 l/min to the welding torch. The shielding gas nitrogen content was increased from 0.5% to 5% in 0.5% increments, and the arc, weld pool and completed weld were examined visually during and after welding to determine the minimum shielding gas nitrogen level associated with the onset of significant bubble formation. This point was characterised by severe degassing, spattering and violent metal expulsion from the molten weld metal. The nitrogen contents of the welds corresponding to the onset of steady-state behaviour in each alloy were determined using inert gas fusion analysis techniques.

3.4 Measuring the weld pool temperature during welding

In order to compare the actual nitrogen content of each weld with the calculated equilibrium nitrogen solubility limit, the weld pool temperature had to be determined. An indication of the temperature of the molten weld metal during welding was obtained by measuring the temperature of the centre of the weld pool, based on the assumption that rapid convection in the weld pool ensures a fairly homogeneous temperature distribution in the molten metal during welding. The temperature measurements were performed by inserting a thermocouple into the weld pool behind the arc during welding. The thermocouple was shielded from exposure to the arc by a ceramic sheath that left only the fused end of the wires uncovered. Accurate placement of the thermocouple in the centre of the pool was facilitated by an adjustable steel guide tube attached to the main body of the welding torch, and the thermoelectric signal from the thermocouple was recorded using a calibrated XY-recorder. An average weld pool temperature of 1,722°C ± 14°C was measured.

4 RESULTS AND DISCUSSION

4.1 The influence of the shielding gas nitrogen content on the weld nitrogen level

The average weld metal nitrogen contents measured in the different samples are given in Table 2, and represented graphically in Figures 2 and 3 for the low and high sulphur alloys, respectively. The equilibrium nitrogen solubility, also shown in Figures 2 and 3, was calculated at the measured weld pool temperature of 1,722°C ± 14°C for each nitrogen partial pressure using Wada and Pehlke's equations and interaction parameters [23].

The influence of nitrogen additions to argon shielding gas on the weld nitrogen content of autogenous welds

Table 2. Average weld metal nitrogen contents of the different welded samples (percentage by mass).

Alloy	Comments	Base metal N content	Weld metal N content for various shielding gas compositions				
			Pure Ar	Ar-1.09%N_2	Ar-5,3%N_2	Ar-9,8%N_2	Ar-24,5%N_2
VFA 657	Low N, low S	0.005%	0.017%	0.082%	0.196%	0.242%	0.257%
VFA 658	Medium N, low S	0.105%	0.105%	0.166%	0.230%	0.245%	0.270%
VFA 659	High N, low S	0.240%	0.216%	0.240%	0.267%	0.265%	0.277%
VFA 752	Low N, high S	0.006%	0.016%	0.082%	0.180%	0.184%	0.194%
VFA 753	Medium N, high S	0.097%	0.118%	0.150%	0.220%	0.230%	0.226%
VFA 755	High N, high S	0.280%	0.271%	0.280%	0.331%	0.325%	0.330%

appears to be consistent with that described in the literature for carbon steels and stainless steels. The weld nitrogen content initially increases as the shielding gas nitrogen content increases, and then reaches a constant steady-state concentration that is independent of the actual nitrogen partial pressure. The weld nitrogen contents exceed the equilibrium solubility at all partial pressures investigated. This is consistent with available literature [12-13, 15-16] and confirms that Sievert's law is not obeyed during arc welding.

The influence of the base metal nitrogen content on the absorption and desorption of nitrogen during welding appears to be dependent on the surface-active element concentration in the weld. In the low sulphur alloys (Fig. 2), an increase in the initial base metal nitrogen level causes an increase in the weld nitrogen content at low nitrogen partial pressures. At higher nitrogen partial pressures, the nitrogen content of the welds approaches a steady-state value that is very similar for all three low sulphur alloys and virtually independent of the base metal nitrogen content. In the case of the high sulphur alloys (Fig. 3), an increase in the base metal nitrogen content results in higher weld nitrogen contents over the entire range of nitrogen partial pressures evaluated, including a significant increase in the steady-state nitrogen concentration. This is contrary to the conclusions of Okagawa *et al.* [6] and Suutala [25] that the nitrogen content of welds is not in fluenced by the base metal nitrogen content. This inconsistency can be attributed to the low base metal nitrogen and sulphur levels in the alloys studied by these authors.

The results shown in Figures 2 and 3 indicate that a high weld metal sulphur content reduces the steady-state nitrogen concentration in the case of the low nitrogen alloys. This suggests that, in the absence of significant amounts of nitrogen in the base metal prior to welding, the surface-active element concentration mainly influences the rate of nitrogen absorption from the arc atmosphere. The sulphur content also has a significant influence on the weld metal nitrogen content in alloys containing high levels of base metal nitrogen, with higher sulphur concentrations leading to considerably higher levels of nitrogen after welding. High base metal nitrogen contents also appear to increase the level of supersaturation in the weld metal over that required for the nucleation of nitrogen bubbles at atmospheric pressure. Since a higher weld sulphur concentration implies increased weld pool surface coverage, the higher nitrogen levels in the presence of higher surface-active element concentrations suggest that the nitrogen desorption reaction is retarded, consistent with the findings of Battle and Pehlke [30] and Katz and King [16]. More of

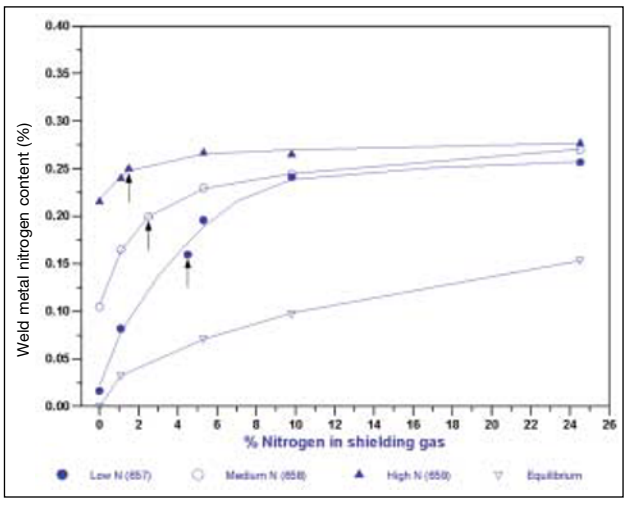

Fig. 2. Weld metal nitrogen concentration as a function of the shielding gas nitrogen content for the experimental *low sulphur* alloys. The arrows indicate the minimum shielding gas compositions where bubbling was observed experimentally.

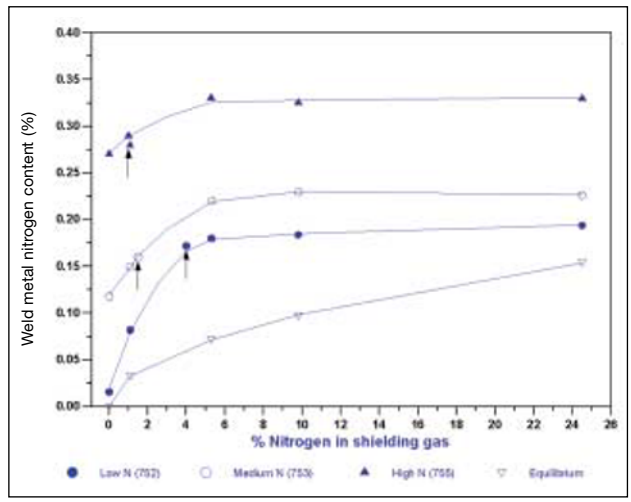

Fig. 3. Weld metal nitrogen concentration as a function of the shielding gas nitrogen content for the experimental *high sulphur* alloys. The arrows indicate the minimum shielding gas compositions where bubbling was observed experimentally.

the nitrogen initially present is therefore maintained in solution and the original nitrogen content is expected to have a more significant influence on the subsequent weld nitrogen concentration (Fig. 3). This is consistent with the results of Arata *et al.* [26], who showed that the total weld metal nitrogen content is the sum of the residual nitrogen content of the base metal and any nitrogen picked up from the interaction between the shielding gas and the molten weld metal. The influence of sulphur on the nitrogen desorption rate is expected to be stronger than on the absorption rate, since nitrogen evolution requires two surface sites for the recombination of nitrogen atoms to form N_2, whereas the absorption of monatomic nitrogen from the arc requires only one surface site per atom dissolved.

4.2 The minimum shielding gas nitrogen content that leads to bubble formation in the weld pool

In order to determine the minimum shielding gas nitrogen content necessary to induce steady-state behaviour, and consequently nitrogen bubble formation, in each of the alloys investigated, the shielding gas nitrogen content was increased from 0.5% to 5% in 0.5% increments during welding. Based on visual observations of the arc and weld pool during welding and the appearance of the completed weld, the minimum shielding gas nitrogen contents that lead to nitrogen bubble formation, and the corresponding weld nitrogen contents, are shown in Table 3 for the experimental alloys.

It is evident that the minimum shielding gas nitrogen content required to initiate bubble formation depends on the base metal nitrogen content and the surface-active element concentration. The saturation limit is reached at progressively lower shielding gas nitrogen contents as the base metal nitrogen level increases. This confirms that base metal nitrogen participates in the nitrogen absorption and desorption reactions during welding. Less nitrogen is required in the shielding gas to reach the saturation limit and initiate steady-state behaviour in the high sulphur alloys because an appreciable fraction of the nitrogen already present in the base metal is prevented from escaping by the higher level of surface coverage. A significant amount of the nitrogen present in the base metal prior to welding is therefore available to participate in the nitrogen absorption/desorption reactions in addition to any nitrogen absorbed from the shielding gas during welding.

Table 3. Minimum shielding gas nitrogen content required to initiate steady-state behaviour and bubble formation (percentage by mass).

Alloy	Comments	Minimum shielding gas N content required to initiate degassing	Corresponding weld metal N content
VFA 657	Low N, low S	4.5%	0.160%
VFA 658	Medium N, low S	2.5%	0.200%
VFA 659	High N, low S	1.5%	0.250%
VFA 752	Low N, high S	4.0%	0.172%
VFA 753	Medium N, high S	1.5%	0.160%
VFA 755	High N, high S	1.0%	0.290%

5 KINETIC MODEL OF NITROGEN ABSORPTION AND DESORPTION DURING WELDING

In order to justify the conclusions reached in the first phase of this investigation, a suitable theoretical framework is needed. Although a number of thermodynamic models have been developed for nitrogen absorption and desorption during welding, most of these models were derived for pure iron or low-alloy steel welds. Results reported by Kuwana *et al.* [24] suggest that higher chromium contents influence nitrogen absorption/desorption by increasing the equilibrium nitrogen solubility limit in steel. More nitrogen can dissolve in the steel during welding, and reaction rates therefore play an increasingly important role. This suggests that a kinetic approach may be more appropriate than a thermodynamic method for describing the dissolution of nitrogen in high chromium alloy and stainless steel welds. A kinetic model was therefore developed to quantify the effect of the shielding gas nitrogen content, the base metal nitrogen content prior to welding, and the weld metal surface-active element concentration on nitrogen absorption and desorption during the autogenous arc welding of stainless steel.

5.1 Outline of the kinetic model

The proposed kinetic model is illustrated schematically in Fig. 4, and was developed on the basis of the following assumptions:

a) Nitrogen enters the molten weld pool from two sources:

– the arc atmosphere, i.e. the dissolution of monatomic and diatomic nitrogen from the arc plasma into the liquid metal, and

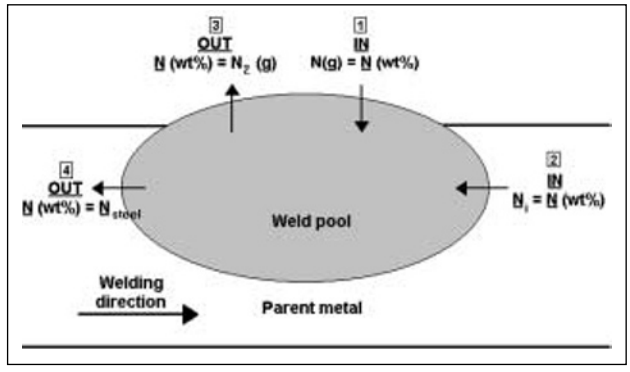

Fig. 4. Schematic illustration of the proposed kinetic model for the absorption and desorption of nitrogen from autogenous stainless steel weld metal.

– the nitrogen-containing base metal that melts at the leading edge of the weld pool during welding.

b) Dissolved nitrogen is removed from the weld pool by:
– recombining to form nitrogen molecules (N_2) that can escape to the atmosphere, and
– solidification of nitrogen-containing weld metal at the rear of the weld pool during welding.

c) Under steady-state conditions the amount of nitrogen entering the weld pool is equal to the amount leaving the weld pool per unit time.

d) The molten weld pool is completely covered by plasma using the welding parameters described earlier.

e) The solidification rate at the rear of the pool is proportional to the welding speed.

f) Due to rapid convection in the molten metal, the weld pool is well mixed with a uniform nitrogen concentration. Rapid mass flow also ensures a fairly homogeneous temperature distribution in the molten pool.

g) The model is only valid under conditions where the evolution of nitrogen occurs at the weld pool surface and no bubble formation takes place in the weld metal.

The proposed rate equations for the four nitrogen absorption and desorption processes shown in Fig. 4 are given below.

5.1.1 Nitrogen entering the weld pool from the arc atmosphere

The absorption of monatomic nitrogen from the arc plasma, reaction (1), is best described by a first order rate equation, with the mass transfer rate for this reaction represented by equation (2).

$$N\ (g) \rightarrow \underline{N}\ (wt\%) \tag{1}$$

$$\frac{dm_N}{dt} = Ak\left[N(g) - \frac{N_{steel}}{K}\right] \tag{2}$$

where:

$\underline{N}$ (wt%) refers to nitrogen dissolved in the molten weld metal,

$\frac{dm_N}{dt}$ is the rate of mass transfer of nitrogen ($kg.s^{-1}$),

A is the weld pool surface area (m^2),

k is the reaction rate constant for reaction (1) ($kg.m^{-2}.s^{-1}.atm^{-1}$),

N(g) is the monatomic nitrogen content of the arc (atm),

N_{steel} is the weld nitrogen content (wt%), and

K is the apparent equilibrium constant for reaction (1).

5.1.2 Nitrogen entering the weld metal through nitrogen-containing base metal melting at the leading edge of the pool

If the weld pool has a length L, the time required to melt a volume of metal equal to the volume of the pool is equal to L/v, where v is the torch travel speed. The base metal melting rate (in $kg.s^{-1}$) is then represented by equation (3).

$$\text{Melting rate} = \rho V\left(\frac{v}{L}\right) \tag{3}`$$

where:

ρ is the density of the molten metal ($kg.m^{-3}$), and

V is the weld pool volume (m^3).

The nitrogen mass transfer rate is given by equation (4).

$$\frac{dm_N}{dt} = \frac{N_i\,(wt\%)}{100}\,\rho V\left(\frac{v}{L}\right) \tag{4}$$

where N_i is the initial base metal nitrogen content (wt%).

5.1.3 Nitrogen leaving the weld pool by recombining to form N_2

Nitrogen evolution from the weld metal is represented by equation (5), and the mass transfer rate for this reaction by the second order rate equation (6).

$$2\underline{N}\ (wt\%) \rightarrow N_2\ (g) \tag{5}$$

$$\frac{dm_N}{dt} = -k'\,A\,N_{steel}^{\,2} - K'\,P_{N_2}) \tag{6}$$

where:

k' is the reaction rate constant for reaction (5) ($kg.m^{-2}.s^{-1}.[\%N]^{-2}$),

K' is the apparent equilibrium constant for the reaction: $N_2\ (g) \rightarrow 2\underline{N}\ (wt\%)$, and

PN_2 is the partial pressure of N_2 in the atmosphere (atm).

5.1.4 Nitrogen leaving the weld pool through weld metal resolidifying at the rear of the pool

Since the solidification rate at the rear of the pool is equal to the melting rate (equation (3)), the rate at which nitrogen leaves the pool by resolidifying is represented by equation (7).

$$\frac{dm_N}{dt} = -\frac{N_{steel}}{100}\,\rho V\left(\frac{v}{L}\right) \tag{7}$$

Assumption (c) states that the amount of nitrogen entering the weld pool is equal to the amount leaving the weld pool per unit time under steady-state conditions. From the above, it follows that N_{steel} must be equal to the steady-state nitrogen content, N_{ss}, and the total of equations (2) and (4) must be equal to the total of equations (6) and (7) under steady-state conditions:

$$\begin{aligned} &Ak\left[N(g) - \frac{N_{ss}}{K}\right] + \frac{N_i\,(wt\%)}{100}\,\rho V\left(\frac{v}{L}\right) \\ &= Ak'\,[N_{ss}^{\,2} - K'P_{N_2}] + \frac{N_{ss}}{100}\rho V\left(\frac{v}{L}\right) \end{aligned} \tag{8}$$

where N_{ss} is the steady-state nitrogen content (wt%).

Rearranging equation (8) to collect all the terms containing N_{ss} on the left yields equation (9):

$$\begin{aligned} &Ak'\,N_{ss}^{\,2} + \frac{\rho V}{100}\,\frac{v}{L}\,N_{ss} + Ak\,\frac{N_{ss}}{K} \\ &= Ak'\,K'\,P_{N_2} + AkN\,(g) + \frac{v}{L}\,\frac{\rho V}{100}\,N_i\,(wt\%) \end{aligned} \tag{9}$$

For a specific shielding gas composition and set of welding parameters, the weld pool area A, length, L, and volume, V, the monatomic nitrogen content of the arc, N(g), the welding speed, v, the density, ρ, the equilibrium constants, K and K', and the nitrogen partial pres-

sure in the shielding gas, PN_2, should remain constant, regardless of the base metal nitrogen content and the surface-active element concentration in the weld metal. The following conclusions can now be drawn:

According to equation (9), the steady-state nitrogen content, N_{ss}, is a function of the base metal nitrogen content, N_i, with an increase in base metal nitrogen concentration leading to an increase in the steady-state nitrogen content. This was observed experimentally, as shown in Figures 2 and 3. The extent of this dependence, however, is determined by the magnitude of the two reaction rate constants, *k* (for the absorption reaction) and *k'* (for the desorption reaction). Earlier results suggested that the desorption rate constant varies with the surface-active element concentration in the weld metal. In the low sulphur steels, desorption of nitrogen from the weld pool is rapid, leading to high values of *k'*, whereas desorption is retarded in the high sulphur alloys, resulting in low *k'* values. The absorption rate constant, *k*, is not expected to be a strong function of the surface-active element concentration.

Given the low desorption rate constant in the high sulphur alloys, equation (9) suggests that the steady-state nitrogen content is a strong function of the base metal nitrogen content, with N_{ss} increasing as N_i increases. This is consistent with the results shown in Fig. 3. In the low sulphur alloys, *k'* is expected to be higher and gas-metal (or plasma-metal) reactions should therefore play a more significant role in determining the steady-state nitrogen content. According to equation (9), the influence of the base metal nitrogen content on the steady-state weld metal nitrogen level is less pronounced at high *k'* values. This is consistent with the results shown in Fig. 2.

5.2 Values of the constants

In order to use equation (9) to predict the nitrogen content of the experimental alloys after welding, a number of constants, including the partial pressure of monatomic nitrogen in the arc, *N*(g), the weld pool surface area, *A*, volume, *V*, and length, *L*, the density of the molten metal, ρ, the two apparent equilibrium constants for the absorption and desorption reactions, *K* and *K'*, and the two reaction rate constants, *k* and *k'*, have to be determined. The values of these constants were measured experimentally or calculated using relationships obtained from published literature.

5.2.1 Partial pressure of monatomic nitrogen in the arc

The partial pressure of monatomic nitrogen in the arc was estimated using the method developed by Mundra and DebRoy [20] and Palmer and DebRoy [21]. These authors derived equation (11) for calculating the partial pressure of monatomic nitrogen formed as a result of the dissociation of molecular nitrogen, reaction (10), at a hypothetical temperature T_d in the arc plasma. T_d is defined as the dissociation temperature at which the equilibrium thermal dissociation of diatomic nitrogen in the arc would produce the actual partial pressure of monatomic nitrogen present in the plasma. The authors concluded that T_d is approximately 100 K higher than the weld pool surface temperature.

$$1/2\ N_2\ (g) \rightarrow N\ (g) \tag{10}$$

$$P_N = \sqrt{P_{N_2}} \exp\left(-\frac{\Delta G^0_{10,\,Td}}{TR_d}\right) \tag{11}$$

where:

PN is the partial pressure of monatomic nitrogen in the arc (atm),

$\Delta G^0_{10,Td}$ is the standard free energy for reaction (10) at T_d,

and *R* is the universal gas constant (8.314 $J.K^{-1}.mol^{-1}$).

Since the extent of dissociation of diatomic nitrogen is low under typical welding conditions, PN_2 can be assumed to be equal to the partial pressure of N_2 in the inlet gas. The free energy of formation of monatomic nitrogen from N_2, $\Delta G^0_{10,Td}$, used by Mundra and DebRoy [20] and Palmer and DebRoy [21] was obtained from the compilation by Elliott and Gleiser [31]. However, the data in this reference appears to be in error, specifically with regards to the heat of formation of N from N_2. Elliott and Gleiser quote a value of 358.0 kJ/mol (of N), whereas Kubaschewski *et al.* [32] report 472.7 kJ/mol. The latter value agrees exactly with the bond strength of the diatomic molecule of 945.44 kJ/mol (of N_2) [33].

One implication of this is that the conclusion of Palmer and DebRoy that the effective plasma temperature (as regards the dissociation of N_2) is 100°C higher than the metal surface temperature, is in error, because this conclusion was based on the data of Elliott and Gleiser. In the current investigation, this inaccuracy was corrected by recalculating the "effective dissociation temperature" as that temperature which yields – for the conditions of the Palmer and DebRoy experiments – the same partial pressure of monatomic nitrogen when the Kubaschewski *et al.* data are used, as does the Elliott and Gleiser data at a temperature of 1,400°C, which is 100°C higher than the surface temperature in the Palmer and DebRoy investigation. This yields a reassessed effective plasma temperature that is 633°C higher than the surface temperature – much higher than the value reported by Palmer and DebRoy.

If the surface temperature of the weld pool is assumed to be approximately equal to the measured weld pool temperature of 1,722°C, the values of PN_2, $\Delta G^0_{10,Td}$, T_d and *R* can be substituted into equation (11), and the partial pressure of monatomic nitrogen in the arc plasma can be estimated for all the shielding gas atmospheres used in this investigation. The estimated monatomic nitrogen partial pressures are shown in Table 4, taking into consideration that total atmospheric pressure in Pretoria, where the experiments were performed, is 0.86 atm.

5.2.2 The weld pool surface area, A, length, L, and volume, V

The area and length of the weld pool were estimated by assuming that the crater at the end of each weld bead,

Table 4. The estimated monatomic nitrogen partial pressure in the arc atmosphere for an effective plasma temperature of 2,628 K and the equilibrium nitrogen content of the weld metal at a weld pool temperature of 1,722°C as a function of the shielding gas nitrogen content.

Shielding gas nitrogen content	Nitrogen partial pressure, PN_2	Monatomic nitrogen partial pressure, PN	Equilibrium nitrogen content, N_{eq}
1.09%	0.0094 atm	8.43×10^{-8} atm	0.0200 wt%
5.3%	0.0456 atm	1.86×10^{-7} atm	0.0442 wt%
9.8%	0.0843 atm	2.53×10^{-7} atm	0.0601 wt%
24.5%	0.2107 atm	4.00×10^{-7} atm	0.0950 wt%

where insufficient liquid metal was present to fill the depression created by the arc jet, has the same dimensions as the weld pool during welding. In order to determine these dimensions, the end craters of seven weld beads were photographed, and the area and maximum length of each crater were measured. The volume of the weld pool was estimated by sectioning a number of weld beads and photographing polished and etched cross sections. The average values of the weld pool length, area and volume determined using these methods are shown in Table 5.

5.2.3 The apparent equilibrium constants. K and K'

5.2.3.1 The apparent equilibrium constant for the desorption reaction, K'

If nitrogen desorption from the weld pool during welding is represented by equation (5), the apparent equilibrium constant, *K'*, for this reaction is given by equation (12).

$$K' = \frac{[N_{eq}\ (wt\%)]^2}{P_{N_2}} \tag{12}$$

where N_{eq} is the equilibrium N content of the molten metal at the weld pool temperature (wt%).

The equilibrium nitrogen content as a function of temperature can be calculated using Wada and Pehlke's results and equation (13) [23].

$$\log (\underline{N}_{eq}) = -\frac{247}{T} - 1.22 - \left(\frac{4780}{T} - 1.51\right) \log f_{N,\,1873} - \left(\frac{1760}{T} - 0.91\right) (\log f_{N,\,1873})^2 \tag{13}$$

where

T is the temperature (K), and

$f_{N,1873}$ is the nitrogen activity coefficient at 1873 K.

Table 5. Average weld pool dimensions (with 95% confidence interval).

Weld pool surface area	34.1 ± 4.8 mm²
Weld pool length	7.4 ± 0.5 mm
Weld pool volume	63.9 ± 6.3 mm³

The activity coefficient f_N is calculated from the composition of the steel using equation (14) [23].

$$\log f_N = \{-164[\%Cr] + 8.33[\%Ni] - 33.2[\%Mo] - 134[\%Mn] + 1.68[\%Cr]^2 - 1.83[\%Ni]^2 - 2.78[\%Mo]^2 + 8.82[\%Mn]^2 + (1.6[\%Ni] + 1.2[\%Mo] + 2.16[\%Mn]).[\%Cr] + (-0.26[\%Mo] + 0.09[\%Mn]).[\%Ni]\}/T + \{0.0415[\%Cr] + 0.0019[\%Ni] + 0.0064[\%Mo] + 0.035[\%Mn] - 0.0006[\%Cr]^2 + 0.001[\%Ni]^2 + 0.0013[\%Mo]^2 - 0.0056[\%Mn]^2 + (-0.0009[\%Ni] - 0.0005[\%Mo] - 0.0005[\%Mn]).[\%Cr] + (0.0003[\%Mo] + 0.0007[\%Mn]).[\%Ni]\} + 0.13[\%C] + 0.06[\%Si] + 0.046[\%P] + 0.007[\%S] + 0.01[\%Al] - 0.9[\%Ti] - 0.1[\%V] - 0.003[\%W] - 0.12[\%O] \tag{14}$$

where: [%M] is the alloying element content in wt%.

For the experimental alloys, calculation yields the equilibrium nitrogen contents shown in Table 4 at a weld pool temperature of 1,722°C, taking into consideration that total atmospheric pressure in Pretoria is 0.86 atm. These values were substituted into equation (12) to yield an average apparent equilibrium constant of 4.28×10^{-2} for the nitrogen desorption reaction.

5.3.2.2 The apparent equilibrium constant for the absorption reaction, K

The apparent equilibrium constant, *K,* for the nitrogen dissolution reaction (equation (1)) is represented by equation (15). The relationship between *K, K'* and K_1 (the equilibrium constant for the dissociation of diatomic nitrogen) is shown in equation (16) with the equilibrium constant, K_1, for nitrogen dissociation (reaction (10)) given by equation (17).

$$K = \frac{N_{eq}}{P_N} \tag{15}$$

where N_{eq} is the nitrogen concentration in equilibrium with the monatomic nitrogen in the arc.

$$K = \frac{\sqrt{K'}}{K_1} \tag{16}$$

where:

$$K_1 = \frac{P_N}{\sqrt{P_{N_2}}} \tag{17}$$

Since PN_2 and *K'* are known, and the partial pressure of monatomic nitrogen in the arc plasma at the weld pool temperature can be determined, *K* can be calculated. Calculation yields an average *K* value of 2.55×10^8 at the weld pool temperature of 1,722°C. K_1, the equilibrium constant of reaction (10), was calculated from the data of Kubaschewski *et al.* [32].

5.2.4 The nitrogen desorption and absorption rate constants, k' and k

5.2.4.1 The nitrogen desorption rate constant, k'

Correlations based on the reaction rate of diatomic nitrogen with pure iron from the summaries of Belton [34] and Turkdogan [35] were used to estimate the rate constant for nitrogen desorption from the weld pool as N_2 (reaction (5)). For the reaction $N_2(g) \rightarrow 2\underline{N}(wt\%)$, the rate constant (for temperatures ranging from 1,550°C to 1,700°C) is given by equation (18):

$$k_1 = \frac{10^{(-6340/T + 1.85)}}{1 + 260\, f_o\, [\%O] + 130\, f_S\, [\%S]} \ g.cm^{-2} . min^{-1} . atm^{-1} \quad (18)$$

where:

f_O and f_S are the activity coefficients of dissolved oxygen and sulphur, respectively, and [%O] and [%S] are the mass percentages of dissolved oxygen and sulphur, respectively.

The rate expression used with this rate constant is as follows:

$$\frac{dm_N}{dt} = k_1 A \left[P_{N_2} - \frac{N_{steel}^{\ 2}}{K'} \right] \quad (19)$$

Comparison with equation (6) shows that $k' = k_1/K'$.

For stainless steels, the activity coefficient of sulphur, f_S, can be estimated as follows (36):

$$\log f_S = [\%Cr] \left(-\frac{94.2}{T} + 0.040 \right) \quad (20)$$

For a weld pool temperature of 1,722°C and an average chromium content of 24.4%, this yields a value of f_S = 0.67 for the experimental alloys.

In these calculations, the effect of dissolved oxygen on the rate constant was neglected, since no data were available on oxygen levels. However, the activity of oxygen is expected to be low in chromium-rich steels, and since the sulphur levels are comparatively high, neglecting the effect of dissolved oxygen is not expected to affect the calculations significantly.

Substitution of the constants and unit conversion yields the following expression for the rate constant, for a temperature of 1,722°C:

$$k' = \frac{0.183}{1 + 87\, [\%S]} \ kg . m^{-2} . s^{-1} . (\%)^{-2} \quad (21)$$

This expression for the desorption rate constant is valid for liquid iron. For stainless steels, the rate constant for this reaction is generally larger than that for liquid iron by a factor of about 6 [34, 37]. However, this conclusion is based on experiments conducted at 1,600°C, and leads to an overestimate in this investigation. Part of the reason for choosing not to increase the rate constant over that for pure iron is illustrated in Fig. 5, which compares the measured and predicted reduction in the weld nitrogen content for welding under pure argon. When welding in pure argon, no monatomic nitrogen is assumed to form in the plasma, and hence the (unknown) absorption rate constant *k* has no effect on the weld nitrogen content that is calculated using equation (9). As the figure shows, both values of the rate constant *k'* overpredict the decrease in the weld nitrogen content, but the correspondence is much better for the smaller rate constant.

Based on these conclusions, equation (21) yields values for the desorption rate constant, *k'*, of 6.28×10^{-2} and 3.21×10^{-2} kg.m^{-2}.s^{-1}.(%)$^{-2}$ for the low and high sulphur alloys, respectively. The reduction in the desorption rate constant at higher surface-active element concentrations is consistent with a site blockage model, where sulphur atoms are assumed to occupy a fraction of the surface sites required for the adsorption of nitrogen.

5.4.2.2 The nitrogen absorption rate constant, k

No literature data on the value of the rate constant *k* for the reaction of monatomic nitrogen with stainless steel was found. This constant was therefore estimated from the experimental data, using equation (9) for the case where the shielding gas contained 1.09% nitrogen (nitrogen bubbles formed at higher nitrogen contents, rendering one of the assumptions on which the model is based invalid). Calculated values of the absorption rate constant are summarised in Table 6.

As shown in this table, use of the larger rate constant *k'* yields values for the constant *k* which seem to depend on the initial nitrogen content of the steel. There appears

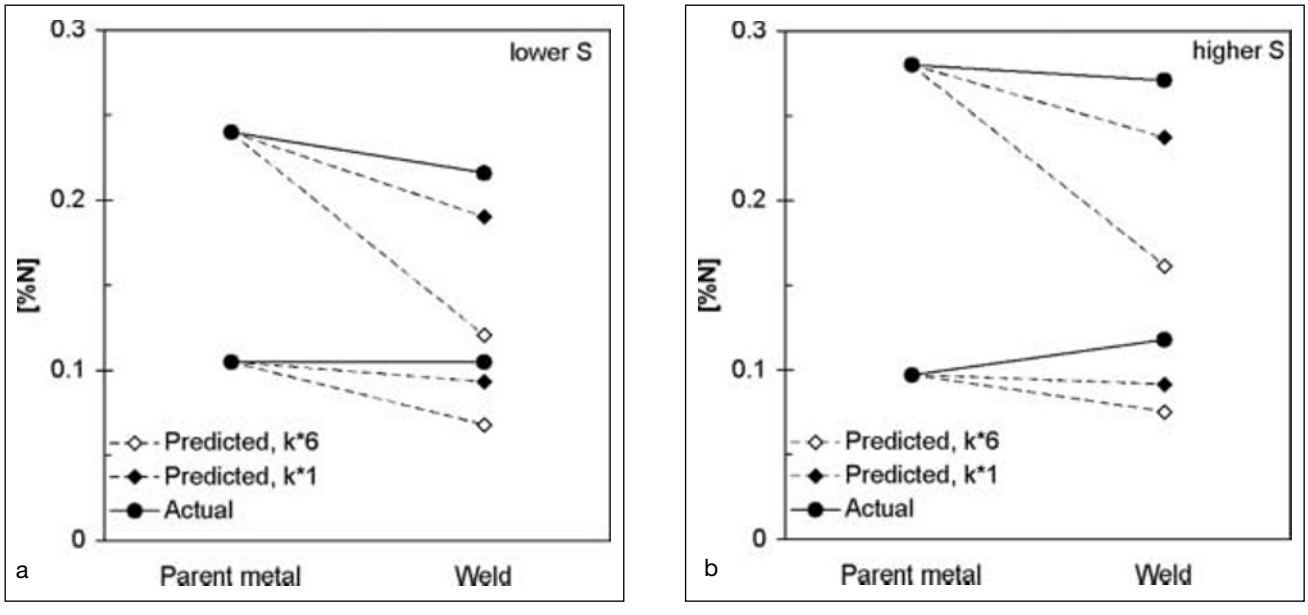

Fig. 5. Comparison of the actual decrease in nitrogen content from the original base metal composition (filled circles), with the calculated decrease using the rate constant for liquid iron (filled diamonds), and for the case where this rate constant is increased by a factor of 6 (open diamonds). Results are shown for a) the low sulphur and b) the high sulphur steels, in both cases for welding in pure argon.

Table 6. Calculated values of the rate constant *k* for the absorption of dissociated nitrogen by the weld pool.

a) Rate constant *k'* for liquid iron.

Alloy	Comments	Base metal nitrogen content	Sulphur content	$10^{-3}k$ (kg.m^{-2}.s^{-1}.atm^{-1})
VFA 657	Low N. low S	0.005	0.023	38
VFA 658	Medium N. low S	0.105	0.023	43
VFA 659	High N. low S	0.240	0.022	35
VFA 752	Low N. high S	0.006	0.052	36
VFA 753	Medium N. high S	0.097	0.061	30
VFA 755	High N. high S	0.280	0.049	27

b) Rate constant *k'* taken to be 6 times that for liquid iron.

Alloy	Comments	Base metal nitrogen content	Sulphur content	$10^{-3}k$ (kg.m^{-2}.s^{-1}.atm^{-1})
VFA 657	Low N. low S	0.005	0.023	57
VFA 658	Medium N. low S	0.105	0.023	124
VFA 659	High N. low S	0.240	0.022	210
VFA 752	Low N. high S	0.006	0.052	46
VFA 753	Medium N. high S	0.097	0.061	61
VFA 755	High N. high S	0.280	0.049	159

to be no fundamental reason why this should be the case. When the rate constant *k'* for liquid iron is used in its original form, the rate constant *k* is approximately the same for all the steels. Interestingly, no strong effect of the sulphur content on the rate constant for dissociated nitrogen was found. This is in contrast with the case for the reaction which involves molecular nitrogen, where an increase in sulphur from 0.022% to 0.054% causes a decrease in the rate constant *k'* by a factor of approximately 2. Given the weak dependence of *k* on steel composition, an average value of 3.5×10^4kg.m^{-2}.s^{-1}.atm^{-1} was used in the subsequent calculations (together with the value of *k'* as for liquid iron).

5.2.5 Summary of the constants required in equation (9)

A summary of all the constants required for substitution into equation (9) is given in Table 7.

Table 7. Summary of the constants required in equation (9).

Constant	Value
PN	8.43×10^{-8} atm if PN_2 = 0.0094 atm 1.86×10^{-7} atm if PN_2 = 0.0456 atm 2.53×10^{-7} atm if PN_2 = 0.0843 atm 4.00×10^{-7} atm if PN_2 = 0.2107 atm
A	34.1 mm^2
L	7.4 mm
V	63.9 mm^3
K	2.55×10^8
K'	4.28×10^{-2}
r	6,755 kg.m^{-3}
n	2.7 mm.s^{-1}
k	3.5×10^4 kg.m^{-2}.s^{-1}.atm^{-1}
k'	6.28×10^{-2} kg.m^{-2}.s^{-1}.(%)$^{-2}$ for the low sulphur alloys 3.21×10^{-2} kg.m^{-2}.s^{-1}.(%)$^{-2}$ for the high sulphur alloys

5.3 Predicted weld nitrogen concentration

Figure 6 shows the predicted weld nitrogen concentration as a function of the shielding gas nitrogen content for the experimental alloys. The predicted behaviour is close to that found experimentally (shown in Figures 2 and 3), with marked increases in weld nitrogen content at low nitrogen partial pressures. The influence of the base metal nitrogen content and the surface-active element concentration is also consistent with that observed experimentally.

The results shown in Figure 6 are only valid until the onset of bubble formation. Beyond this point, nitrogen is

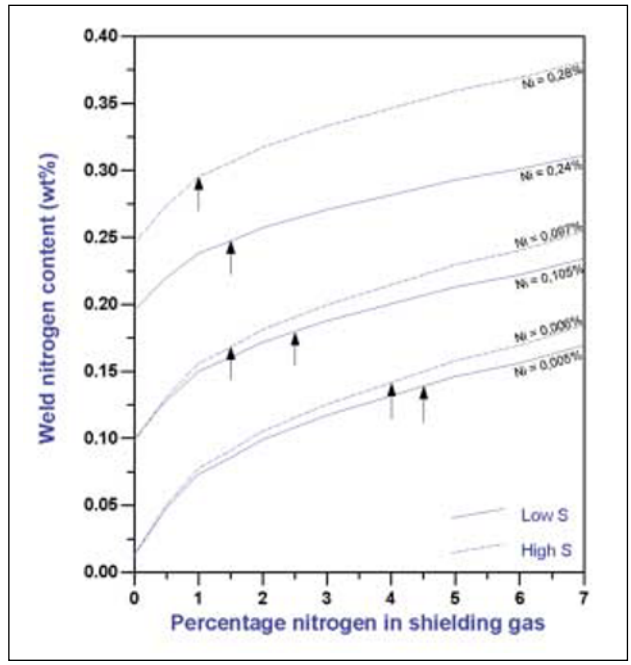

Fig. 6. Predicted change in the weld nitrogen contents of the experimental alloys for shielding gases that are increasingly rich in nitrogen. The arrows indicate the minimum shielding gas compositions where bubbling was observed.

removed from the weld pool not only by the gas-metal reaction at the weld pool surface, but also by bubble formation within the pool. This condition is not covered by the simple kinetic model presented here. For shielding gas compositions at the onset of bubbling, the predicted rates at which nitrogen enters and leaves the pool by means of the four mechanisms considered in the model are summarised in Table 8. This shows that the main mechanism by which nitrogen enters the pool is a function of the initial base metal nitrogen content, with nitrogen absorption from the arc playing a dominant role at low base metal nitrogen contents, and melting of nitrogen-containing base metal at high initial nitrogen levels. The main exit mechanism appears to be nitrogen leaving the weld metal through solidification, rather than nitrogen desorption to the atmosphere. It is evident from Fig. 6 that higher sulphur concentrations slightly retard the desorption of N_2 to the atmosphere (giving higher nitrogen contents in the weld pool for a similar base metal nitrogen content). This is consistent with the site blockage model described earlier.

Two factors are of interest in the practical welding situation: the change in nitrogen content upon welding, and the formation of nitrogen bubbles. The former situation appears to be fairly well described by the kinetic model. However, the latter is more difficult to predict. As Figures 2 and 3 show, bubble formation was observed for weld nitrogen contents ranging from 0.16% to 0.29%. In comparison, the equilibrium nitrogen content for a nitrogen partial pressure of 0.86 atm (atmospheric pressure in Pretoria) is 0.19% at 1,722°C. (The saturation concentration depends somewhat on temperature).

For the formation of a nitrogen bubble in the weld pool, the nitrogen partial pressure within the bubble must at least equal atmospheric pressure (in fact, it must be slightly higher to compensate for the surface tension of the bubble). Considering that the nitrogen saturation content is 0.19%, the high nitrogen alloys display a significant degree of supersaturation prior to the onset of bubble formation. This is consistent with the results of Blake and Jordan [14], who reported that the steady-state nitrogen content of molten iron is in excess of that required to provide an internal pressure of one atmosphere at the assumed temperature of the liquid metal. The increased levels of supersaturation for the higher-nitrogen alloys are presumably related to the higher rate of nitrogen removal as N_2 at the onset of bubble formation (as is evident from Table 8). Given that nitrogen bubble formation and detachment require bubble nucleation and growth, it appears reasonable to assume that a higher nitrogen removal rate (as bubbles) would require a higher degree of supersaturation (a larger "driving force"). Such a link between supersaturation and the nitrogen removal rate is also evident in the experimental results shown in Figures 2 and 3, where the weld nitrogen concentration increases if the shielding gas nitrogen content is increased beyond the onset of bubble formation.

On the other hand, it does not appear possible to form bubbles at weld nitrogen contents below 0.19%, as was found experimentally for most of the lower nitrogen alloys. Possible reasons for this discrepancy include deviation of the weld pool temperature from that measured, deviation of the actual saturation concentration of nitrogen from that predicted by the correlation for f_N, and errors in chemical analysis.

6 CONCLUSIONS

– Nitrogen absorption and desorption reactions in the presence of nitrogen-containing shielding gas during the autogenous welding of stainless steel do not obey Sievert's law. The weld metal nitrogen content initially increases with an increase in the shielding gas nitrogen content at low nitrogen partial pressures. At higher partial pressures a dynamic equilibrium is created where the amount of nitrogen absorbed by the weld metal is balanced by the amount of nitrogen evolved from the weld pool during welding.

– The nitrogen content of autogenous stainless steel welds is a function of the nitrogen partial pressure in the shielding gas, the base metal nitrogen content and the surface-active element concentration in the weld metal. In alloys with low surface-active element concentrations, the steady-state nitrogen content of the weld metal is not influenced to any significant extent by the base metal nitrogen content. In the case of alloys with high surface-active element concentrations, an increase in the base metal nitrogen content results in higher weld metal nitrogen contents over the entire range of nitrogen partial pressures evaluated, including a significant

Table 8. The relative contributions of the four reactions that add or remove nitrogen to or from the weld pool. at the respective shielding gas compositions where bubble formation was observed experimentally.

Alloy	Comments	$\frac{dN(wt\%)}{dt}$. mg.s^{-1}			
		(1) Absorption of monatomic N from plasma	(2) Melting of base metal at leading edge of weld pool	(3) Desorption of N_2 from the weld pool	(4) Solidification at the rear of the weld pool
VFA 657	Low N, low S	0.203	0.008	- 0.025	- 0.185
VFA 658	Medium N, low S	0.151	0.165	- 0.055	- 0.261
VFA 659	High N, low S	0.116	0.378	- 0.120	- 0.374
VFA 752	Low N, high S	0.191	0.009	- 0.014	- 0.187
VFA 753	Medium N, high S	0.117	0.153	- 0.024	- 0.246
VFA 755	High N, high S	0.095	0.441	- 0.093	- 0.442

increase in the steady-state nitrogen concentration. It is postulated that the surface-active element concentration in the weld metal influences the nitrogen absorption and desorption rates by occupying surface sites required for the absorption of monatomic nitrogen from the arc plasma and the recombination of nitrogen atoms to form N_2 (desorption).

– The minimum shielding gas nitrogen content required to induce steady-state behaviour and nitrogen bubble formation in the experimental alloys is also a function of the base metal nitrogen content of the alloy and the surface-active element concentration. The weld metal saturation limit is reached at progressively lower shielding gas nitrogen contents as the base metal nitrogen level increases. It is postulated that less nitrogen is required in the shielding gas to reach the saturation limit in the high sulphur alloys because an appreciable fraction of the nitrogen already present in the base metal is prevented from escaping by the higher level of surface coverage.

– A kinetic model can be used to describe nitrogen absorption and desorption during the welding of the experimental stainless steels. The proposed model considers the absorption of monatomic nitrogen from the arc plasma, the evolution of N_2 from the weld pool, nitrogen entering the weld metal through the melting of nitrogen-containing base metal, and nitrogen leaving the weld pool through the solidification of weld metal at the rear of the pool. The predictions of the model show good agreement with the experimental results.

– The calculated nitrogen desorption rate constant is a function of the surface-active element concentration in the alloy, with the rate constant decreasing at higher concentrations of sulphur in the steel. This is consistent with a site blockage model, where surface-active elements occupy a fraction of the surface sites required for nitrogen adsorption. The rate constant for the absorption of dissociated nitrogen is, however, not a strong function of the surface-active element concentration.

– The main mechanism by which nitrogen enters the weld pool is dependent on the initial nitrogen content of the alloy, with nitrogen absorption from the arc plasma playing a dominant role at low base metal nitrogen contents, and the melting of nitrogen-containing base metal at high initial nitrogen levels. The main exit mechanism appears to be nitrogen leaving the pool due to the solidification of nitrogen-containing weld metal at the rear of the weld pool, rather than nitrogen desorption to the atmosphere as N_2.

– Although the minimum shielding gas nitrogen content that leads to bubbling cannot be determined from the model, it is evident that some supersaturation above that required to nucleate nitrogen bubbles in the melt occurs in the high nitrogen alloys. This can probably be attributed to the higher rate of nitrogen removal as N_2 at the onset of bubble formation.

7 PRACTICAL IMPLICATIONS

Nitrogen losses from nitrogen-alloyed stainless steels can be expected during autogenous welding in pure argon shielding gas. Small amounts of nitrogen can be added to the shielding gas to counteract this effect, but this should be done with care to prevent bubble formation. Supersaturation before bubble formation does, however, extend the range of shielding gas compositions that can be used.

Higher concentrations of surface-active elements maintain more of the base metal nitrogen originally present in the alloy in solution in the weld pool. Higher sulphur contents also increase the steady-state nitrogen content and the amount of nitrogen that can be accommodated prior to nitrogen bubble formation. Although higher sulphur contents may not be viable in practice, small amounts of oxygen added to the shielding gas during welding will have a similar effect.

Although the kinetic model described in this publication was derived for a series of experimental austenitic stainless steels, its application can probably be extended to other austenitic alloys by considering the influence of composition on the equilibrium nitrogen content and the desorption rate constant. Further work is needed to determine the influence of welding parameters on nitrogen absorption and desorption.

ACKNOWLEDGEMENTS

Special thanks to Columbus Stainless for sponsoring the project and performing the nitrogen analyses and the University of Pretoria for providing laboratory facilities. The assistance of Johann Borman and Karin Frost is also gratefully acknowledged.

REFERENCES

1. Lancaster, J.F. 1999. Metallurgy of welding. Cambridge, Abington Publishing.

2. Franks, R., Binder, W.O., and Thompson, J. 1955. Austenitic chromium-manganese-nickel steels containing nitrogen. Transactions of the American Society for Metals 47: 231 to 266.

3. Schaeffler, A.L. 1949. Constitution diagram for stainless steel weld metal. Metal Progress 56 (11): 680 to 680B.

4. Reed, R.P. March 1989. Nitrogen in austenitic stainless steels. JOM: 16 to 21.

5. Zackay, V.F., Carlson, J.F., and Jackson, P.L. 1956. High nitrogen austenitic Cr-Mn steels. Transactions of the ASM 8: 508 to 525.

6. Okagawa, R.K., Dixon, R.D., and Olson, D.L. 1983. The influence of nitrogen from welding on stainless steel weld metal microstructures. Welding Journal 62 (8): 204s to 209s.

7. Janik-Czachor, M., Lunarska, E., and Szklarska-Smialowska, Z. 1975. Effect of nitrogen content in a 18Cr-5Ni-10 Mn stainless steel on the pitting susceptibility in chloride solutions. Corrosion 31 (11): 394 to 398.

8. Ogawa, T., Aoki, S., Sakamoto, T., and Zaizen, T. 1982. The weldability of nitrogen-containing austenitic stainless steel: Part I – Chloride pitting corrosion resistance. Welding Journal 6 (5): 139 to 148.

9. Mozhi, T.A., Clark, W.A.T., Nishimoto, K., Johnson, W.B., and MacDonald, D.D. 1985. The effect of nitrogen on the sensitisation of AISI 304 stainless steel. Corrosion 41 (10): 555 to 559.

10. Beneke, R., and Sandenbergh, R.F. 1989. The influence of nitrogen and molybdenum on the sensitisation properties of low-carbon austenitic stainless steels. Corrosion Science 29 (5): 543 to 555.

11. Blake, P.D. April 1979. Nitrogen in steel weld metals. Metal Construction: 196 to 197.

12. Lakomskii, V.I., and Torkhov, G.F. 1969. Absorption of nitrogen from a plasma by liquid metal. Soviet Physics – Doklady 13 (11): 1159 to 1161.

13. Kuwana, T., and Kokawa, H. 1986. The nitrogen absorption of iron weld metal during gas tungsten arc welding. Transactions of the Japan Welding Society 17 (1): 20 to 26.

14. Blake, P.D., and Jordan, M.F. March 1971. Nitrogen absorption during the arc melting of iron. Journal of the Iron and Steel Institute: 197 to 200.

15. Den Ouden, G., and Griebling, O. 1989. Nitrogen absorption during arc welding. Proc. 2nd Int. Conf. Trends in Weld. Res. pp. 431-435. ASM International.

16. Katz, J.D, and King, T.B. 1989. The kinetics of nitrogen absorption and desorption from a plasma arc by molten iron. Metallurgical Transactions B 20B: 175 to 185.

17. Bandopadhyay, A., Banerjee, A., and DebRoy, T. 1992. Nitrogen activity determination in plasmas. Metallurgical Transactions B 23B: 207 to 214.

18. Gedeon, S.A., and Eagar, T.W. 1991. Thermochemical analysis of hydrogen absorption in welding. Welding Journal 69 (7): 264s to 271s.

19. Gedeon, S.A. 1987. Hydrogen assisted cracking of high strength steel welds. PhD dissertation, Boston, MIT.

20. Mundra, K., and DebRoy, T. 1995. A general model for partitioning of gases between a metal and its plasma environment. Metallurgical and Materials Transactions B 26B: 149 to 157.

21. Palmer, T.A., and DebRoy, T. 1996. Physical modeling of nitrogen partition between the weld metal and its plasma environment. Welding Journal 75 (7): 197s to 207s.

22. Pehlke, R.D., and Elliott, J.F. 1960. Solubility of nitrogen in liquid iron alloys. 1. Thermodynamics. Transactions of the Metallurgical Society of AIME 218: 1088 to 1101.

23. Wada, H., and Pehlke, R.D. 1977. Solubility of nitrogen in liquid Fe-Cr-Ni alloys containing manganese and molybdenum. Metallurgical Transactions B 8B: 675 to 682.

24. Kuwana, T., Kokawa, H., and Saotome, M. 1995. Quantitative prediction of nitrogen absorption by steel during gas tungsten arc welding. Proc. 3rd Int. Seminar Numerical Analysis of Weldability.

25 Suutala, N. 1982. Effect of manganese and nitrogen on the solidification mode in austenitic stainless steel welds. Metallurgical Transactions A 13A: 2121 to 2130.

26. Arata, Y., Matsuda, F., and Saruwatari, S. 1974. Varestraint test for solidification crack susceptibility in weld metal of austenitic stainless steels. Transactions of the JWRI 3: 79 to 88.

27. Ogawa, T., Suzuki, K., and Zaizen, T. 1984. The weldability of nitrogen-containing austenitic stainless steel: Part II – Porosity, cracking and creep properties. Welding Journal 63 (7): 213s to 223s.

28. Uda, M., and Ohno, S. 1973. Effect of surface-active elements on nitrogen content of iron under arc melting. Transactions of the National Research Institute of Metallurgy 15 (1): 20 to 28.

29. Sinha, O.P., and Gupta, R.C. 1993. Fe-Cr melt nitrogenation when exposed to nitrogen plasma. ISIJ International 33 (5): 567 to 576.

30. Battle, T.D., and Pehlke, R.D. 1986. Kinetics of nitrogen absorption and desorption by liquid iron and iron alloys. Ironmaking & Steelmaking 13 (4): 176 to 189.

31. Elliott, J.F., and Gleiser, M. 1963. Thermochemistry for Steelmaking I. p. 75, Reading, Addison-Wesley.

32. Kubaschewski, O., Alcock, C.B., and Spencer, P.J. 1993. Materials Thermochemistry. Oxford Pergamon Press.

33. Weast, R.C. 1981. CRC Handbook of Chemistry and Physics. Boca Raton, Florida, CRC Press.

34. Belton, G.R. 1993. How fast can we go? The status of our knowledge of the rates of gas-liquid metal interactions. Metallurgical Transactions B 24B: 241-258.

35. Turkdogan, E.T. 1996. Fundamentals of Steelmaking. London, The Institute of Materials.

36. The 19th Committee on Steelmaking, The Japan Society for the Promotion of Science. 1988. Steelmaking data sourcebook. New York, Gordon and Breach.

37. Fruehan, R.J. Nitrogen control in chromium steels. INFACON 6. Proc. 1st Int. Chromium Steel and Alloy Congress, pp. 35-41. SAIMM.